1

A Review on Main Defects of TG-43

Mehdi Zehtabian[1], Reza Faghihi[1,2] and Sedigheh Sina[1,2]
[1]*Nuclear Engineering Department, School of Mechanical Engineering, Shiraz University,*
[2]*Radiation Research Center, School of Mechanical Engineering, Shiraz University,*
Iran

1. Introduction

The Sivert integral and modular dose calculation models (TG-43) are two methods used for calculation of dose distributions around a brachytherapy source (Khan, 2003). Among all methods used for calculation of dose distributions, TG-43 has become most popular and most promising method because it uses the quantities measured in the medium to calculate dose rates.

In this chapter, we will explain the TG-43 dose calculation formalism and after verification of the main reason of its popularity, we will review main defects of this formalism.

1.1 TG-43 formalism

In 1995, the American Association of Physicists in Medicine (AAPM)) published a report on the dosimetry of sources used in interstitial brachytherapy, Task Group No. 43 (TG-43) (Nath et al., 1995). This report introduces dose calculation formalism utilizing new quantities like air kerma strength (S_K), dose rate constant (Λ), geometry function (G (r,θ)), radial dose function (g (r)), and anisotropy function (F (r,θ)). These dosimetry parameters consider geometry, encapsulation and self-filtration of the source, the spatial distribution of radioactivity within the source, and scattering in water surrounding the source. According to this protocol, the absorbed dose rate distribution around a sealed brachytherapy source at point P with polar coordinates (r, θ) can be determined using the following formalism:

$$D(r,\theta) = \Lambda\, S_k\, \frac{\mathrm{G}\,(\mathrm{r},\theta)}{\mathrm{G}\,(\mathrm{r}_0,\theta_0)}\, g(r) F\,(r,\theta) \tag{1}$$

where r is the distance to the point P and θ is the angle with respect to the long axis of the source, and (r_0, θ_0) is reference point that r_0= 1 cm and $\theta_0 = \pi/2$ (Fig. 1).

1.1.1 Air kerma strength

Air kerma strength, S_k, acounts for brachytherapy source strength and is defined as the product of air kerma rate at a calibration distance (d) in free space, which is usually chosen to be 1 m, along the transverse axis of the source and the square of the distance (d^2),

$$S_k = K\,(d) d^2 \tag{2}$$

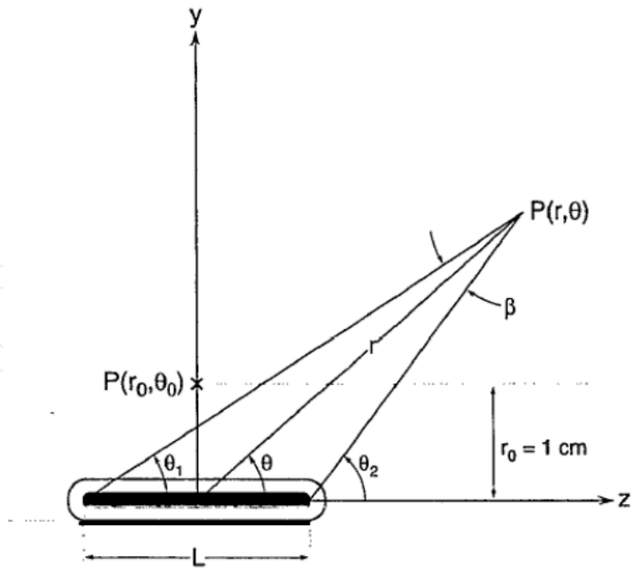

Fig. 1. The geometry of brachytherapy sources used in TG-43 formalism (Nath et al., 1995).

Where K (d) is the air kerma rate, and d is the calibration distance (d). The unit of S_K is U (1 U =1 cGy cm^2 h^{-1}).

1.1.2 Dose rate constant

Dose rate constant, Λ, is defined as dose rate at 1 cm along transverse axis ($\theta_0=\pi/2$) of the source per unit air kerma strength (U) in a water phantom. Dose rate constant of a brachytherapy source is obtained as below:

$$\Lambda = \dot{D}\,(r_0, \theta_0)/S_k \tag{3}$$

Λ has units of cGy h^{-1} U^{-1}. As indicated in Task Group No. 43, the effects of source geometry, the spatial distribution of radioactivity within the source, encapsulation, and self-filtration within the source and scattering in water surrounding the source is considered by this parameter.

1.1.3 Geometry function

Spatial distribution of radioactivity within the source and the slump of the photon fluence with distance from the source are considered by Geometry function, G (r, θ), with the unit of cm^{-2}.

For point sources, the geometry function indicates the inverse square law.

$$G(r,\theta) = \begin{cases} r^{-2}, Point\ source \\ \dfrac{\beta}{Lr\ sin\theta}, Line\ source \end{cases} \tag{4}$$

As it is shown in Figure 1, L is the source active length and $\beta = \theta_2 - \theta_1$ is the angle covering active source from the point (r, θ).

1.1.4 Radial dose function

Radial dose function, g (r), takes into account slump of dose rate arising from absorption and scattering in the medium on the transverse axis of the source and can be affected by self filtration, and encapsulation.

According to AAPM Task Group 43, radial dose function is defined as:

$$g(r) = \frac{D\cdot(r,\theta_0)G(r_0,\theta_0)}{D\cdot(r_0,\theta_0)G(r,\theta_0)} \tag{5}$$

This quantity is defined just on transverse axis, i.e., $\theta_0=\pi/2$. As it is obvious from equation 9.5, effect of the geometric falloff of the photon fluence with distance from the source (inverse square law) has been suppressed by G (r_0, θ_0)/G (r, θ_0).

1.1.5 Anisotropy function

Angular variation of photon absorption and scattering in the encapsulation and the medium at different distances and angles from the source is taken into account by Anisotropy function, F (r, θ).

$$F(r,\theta) = \frac{D\cdot(r,\theta)G(r,\theta_0)}{D\cdot(r,\theta_0)G(r,\theta)} \tag{6}$$

Where $\theta_0=\pi/2$.

Like g (r), applying geometry function in above equation is suppressing the effect of inverse square law on the dose distribution around the source.

Since the publication of TG-43 formalism, many investigations have been performed on determination of the dosimetry parameters of brachytherapy sources and verification of its advantages and limitations of this protocol (Liu et al.,2004; Meigooni et al., 2003, 2005; Melhus & Rivard, 2006; Parsai et al., 2009; Rivard et al., 2004, 2007; Sina et al., 2007, 2009, 2011; Song & Wu, 2008; Zehtabian et al., 2010).

1.1.6 TG-43U1

An updated version of TG-43 (named TG-43U1) protocol were published on 2004, adding several corrections to the original protocol (Rivard et al., 2004).

$$\dot{D}(r,\theta) = \Lambda\, S_k\, \frac{\mathrm{G_L}\,(\mathrm{r},\theta)}{\mathrm{G_L}\,(\mathrm{r_0},\theta_0)}\, g_L(r) F\,(r,\theta) \tag{7}$$

Equation (9-10) includes additional notation compared with the corresponding equation in the original TG-43 formalism, namely the subscript ''*L*'' has been added to denote the line source approximation used for the geometry function.

The definition of S_k in TG-43U1 differs in two important ways from the original AAPM definition of Sk.

The quantity Air-kerma strength, S_K , is the air-kerma rate, K_δ (*d*), *in vacuo* and due to photons of energy greater than δ, at distance *d* from , multiplied by the square of the

distance which should be located on the transverse plane of the source. This distance (*d)* can be any distance large relative to the maximum linear dimension of the radioactivity distribution typically of the order of 1 meter.

$$S_k = K_\delta(d) d^2 \tag{8}$$

When S_k is obtained experimentally, the measurements should be corrected for photon attenuation and scattering in air and any other medium interposed between the source and detector, as well as photon scattering from any nearby objects including walls, floors, and ceilings (Rivard et al., 2004).

The low-energy or contaminant photons (e.g., characteristic x-rays originating in the outer layers of steel or titanium source cladding) would increase K_δ (*d*) without contributing significantly to dose at distances greater than 0.1 cm in tissue. Therefore a cutoff energy δ (i.e. 5 keV for low-energy photon emitting brachytherapy sources) should be considered in calculating K_δ (*d*).

In TG-43U1 dose-calculation formalism, a subscript X has been added to the notation g (r) and geometry function of the original protocol. This protocol presents tables of both g_P (*r*) (point source approximation) and g_L (*r*) (Line source approximation) values. g_X (*r*) is equal to unity at r_0=1 cm.

$$g_X(r) = \frac{\dot{D}(r,\theta_0) G_X(r_0,\theta_0)}{\dot{D}(r_0,\theta_0) G_X(r,\theta_0)} \tag{9}$$

The 2D anisotropy function, *F* (*r*,θ), is defined as:

$$F(r,\theta) = \frac{\dot{D}(r,\theta) G_L(r,\theta_0)}{\dot{D}(r,\theta_0) G_L(r,\theta)} \tag{10}$$

The definition of 2D anisotropy function is identical to the original TG-43 definition, other than inclusion of a subscript *L*, which is added to geometry function.

Generally the TG-43U1 includes:

a. A revised air-kerma strength (S_K) definition.
b. Not using *apparent activity* for specification of source strength
c. Distance-dependent one-dimensional anisotropy function
d. Guidance on extrapolating tabulated TG-43 parameters to long and short distances
e. Minor correction of the original protocol and its implementation (Rivard et al., 2004).

2. Limitations of TG-43 and TG-43U1 dose calculation formalisms

The dosimetry parameters used in the AAPM TG-43 and TG-43U1 dosimetry formalisms are obtained for a single brachytherapy source located at the center of a fixed volume, homogeneous liquid water phantom (Nath et al., 1995; Rivard et al., 2004, 2007). Consequently, these formalisms does not readily account for several aspects that undermine acquisition of high-quality clinical results (Rivard et al., 2009). Some important limitations of TG-43 and TG-43U1 are listed in the following sections (section 9.3.1 and 9.3.4).

2.1 The dosimetry phantom

As mentioned previously, the TG-43 parameters of a brachytherapy source are obtained in a homogeneous water phantom, but in actual clinical cases, the brachytherapy sources are located inside the tissues of the patients.

The different mass absorption coefficients, radiation scattering and attenuations in materials with different compositions would alter the dose distribution in comparison with water.

For example, the brachytherapy sources are placed inside the soft tissue, which is almost equivalent to water, with some small differences in density, atomic number Z_{eff} and chemical composition. Such differences between the compositions of soft tissue and water may cause some discrepancies between the TG-43 parameters in phantoms made up of such materials.

There are also other tissues inside the human body with more differences in density, atomic number and chemical compositions (i.e. bone, breast, lung, …), for which much more discrepancies are observed in TG-43 parameters compared with water phantom. Table 1, shows the chemical compositions and densities of some tissues according to ICRU 44 (ICRU, 1989).

		bone	4 component soft tissue	Muscle
Density (g/cm3)		0.92	1.04	1.04
Element	Atomic number			
(H_2)	1	6.3984%	10.1172%	10.1997%
(C)	6	27.8%	11.1%	12.3%
(N_2)	7	2.7%	2.6%	3.5%
(O_2)	8	41.0016%	76.1828%	72.9003%
(F)	9			
(Na)	11			0.08%
(Mg)	12	0.2%		0.02%
(Si)	14			
(P)	15	7%		0.2%
(S)	16	0.2%		0.5%
(Cl)	17			
(K)	19			0.3%
(Ca)	20	14.7%		

Table 1. The chemical compositions and densities of some tissues (ICRU, 1989)

The effect of phantom material on dose distribution around brachytherapy sources and TG-43 parameters increases with decreasing the photon energy because of the dependence of photoelectric effect on photon energy and the effective atomic number of the absorbing materials.

The ratios of photon mass absorption coefficient of different tissues (μ_{en} tissue) to the mass absorption coefficient (μ_{en} water) of water ($\left(\frac{\mu_{en}}{\rho}\right)_{water}^{tissue}$) are shown on Table 2 for some energies (20, 30, 100, 300, 600, and 1000 keV).

Energy (keV)	Bone	fat	Muscle
20	4.57	0.56	1.03
30	4.80	0.58	1.04
100	1.12	0.96	1.00
300	0.97	1.00	0.99
600	0.96	1.00	0.99
1000	0.96	1.00	0.99

Table 2. The ratio of mass absorption coefficients of different tissues to water ($\left(\frac{\mu_{en}}{\rho}\right)_{water}^{tissue}$) (Khan, 2003).

As it can be seen from Table 2, the difference between mass absorption coefficients in phantoms are more pronounced sources of low energy photons.

To compare the dose distribution in diffeternt dosimetry phantoms, we performed MCNP4c (UT-Battelle & LLC, 2000) Monte Carlo calculations of The Selectron low dose rate (LDR) Cs-137 pellet sources of Nucletron (Nucletron BV, Netherland) (Nucletron, 1998) in homogeneous cubical water phantom of dimention 30*30*30 cm to obtain the dose distribution around a combination of 10 active pellets inside the cylindrical applicator, and then we repeated the MC simulations for different phantom materials (i.e. bone, muscle and soft tissue). The small cubical lattice of 1 mm dimension was defined in the phantoms in order to score dose distribution around the sources inside homogeneouse phantoms using tally F6.

Figure 2, compares the dose distribution around ten active pellets in a cubical water phantom with the dose distribution in bone phantom. The active spherical sources and inactive pellets along with the components of the cylindrical applicator can be seen on the figure.

According to the results of MC simulations, the percentage difference between the dose in water and bone phantoms at transverse plane of the source, increase by increasing the distance from the source center. For instance the percentage difference between the dose in bone and water at a point located at r=0.5 cm on transverse axis of the source is 3%, but this value increases to 20% at r=10 cm.

The comparison between the dose distribution around Cs-137 pellets in water phantom and other phantoms (soft tissue, and muscle) shows the percentage difference of about 3% at r=10 cm which are less pronounced than the percentage difference between bone and water, this is because of the difference in density and effective atomic numbers of these tissues (see Table 1) which lead to different mass attenuation and absorption coefficient of photons.

Melhus et al 2006 investigated the ratio of g (r) in different phantoms (i.e. ICRU 44, four-component soft tissue, breast, Muscle, and soft tissue) to g (r) in water phantom for different brachytherapy sources (i.e. I-125, Cs-137, Ir-192, Pd-103, and Yb-169) using MCNP5 Monte Carlo code (Melhus & Rivard, 2006).

The ratios of g (r) $_{tissue}$ to g (r) $_{water}$ are shown for different brachytherapy sources are shown in Figure 3 (Melhus & Rivard, 2006).

According to Figure 3, the difference between g (r) $_{tissue}$ and g (r) $_{water}$ increase with decreasing photon energy.

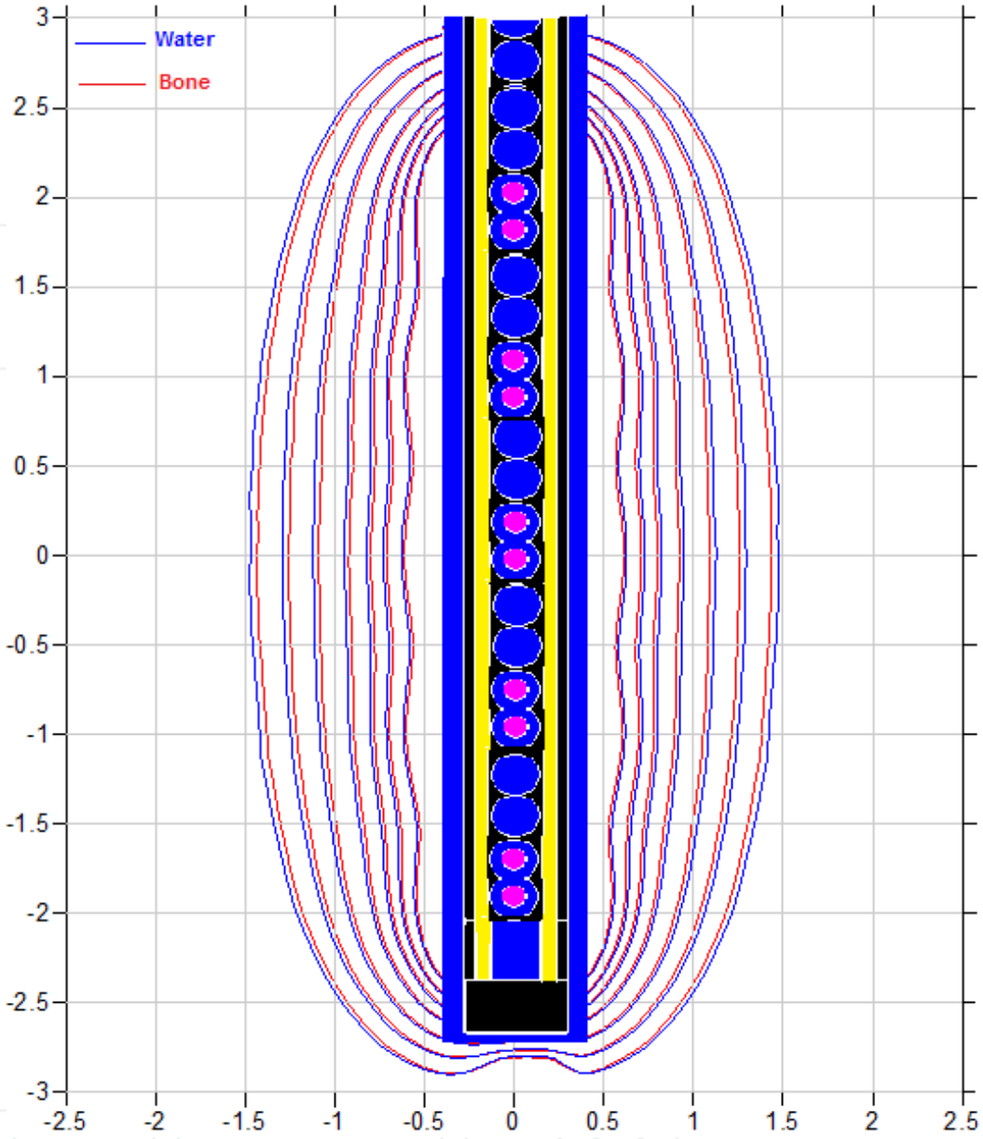

Fig. 2. Comparison of the dose distribution around a combination of 10 Cs-137 active pellets in homogeneous water phantom and bone phantom.

Melhus et al 2006, reported a factor of 2 differences in g (r) between water and ICRU 44 breast tissue for ^{103}Pd at a depth of 9 cm, and the difference of approximately 30% between g (r) for ICRU muscle and soft tissue at a depth of 9 cm for both ^{125}I and ^{103}Pd.

2.2 Inhomogenities

According to the TG-43 dose calculation formalism, the dosimetry is performed in a uniform medium (water) phantom and inhomogenities like bony and soft tissues were not taken into account. There are some implant sites such as head and neck and lung in which the existing inhomogenities are important and would change the dosimetry parameters of the brachytherapy source.

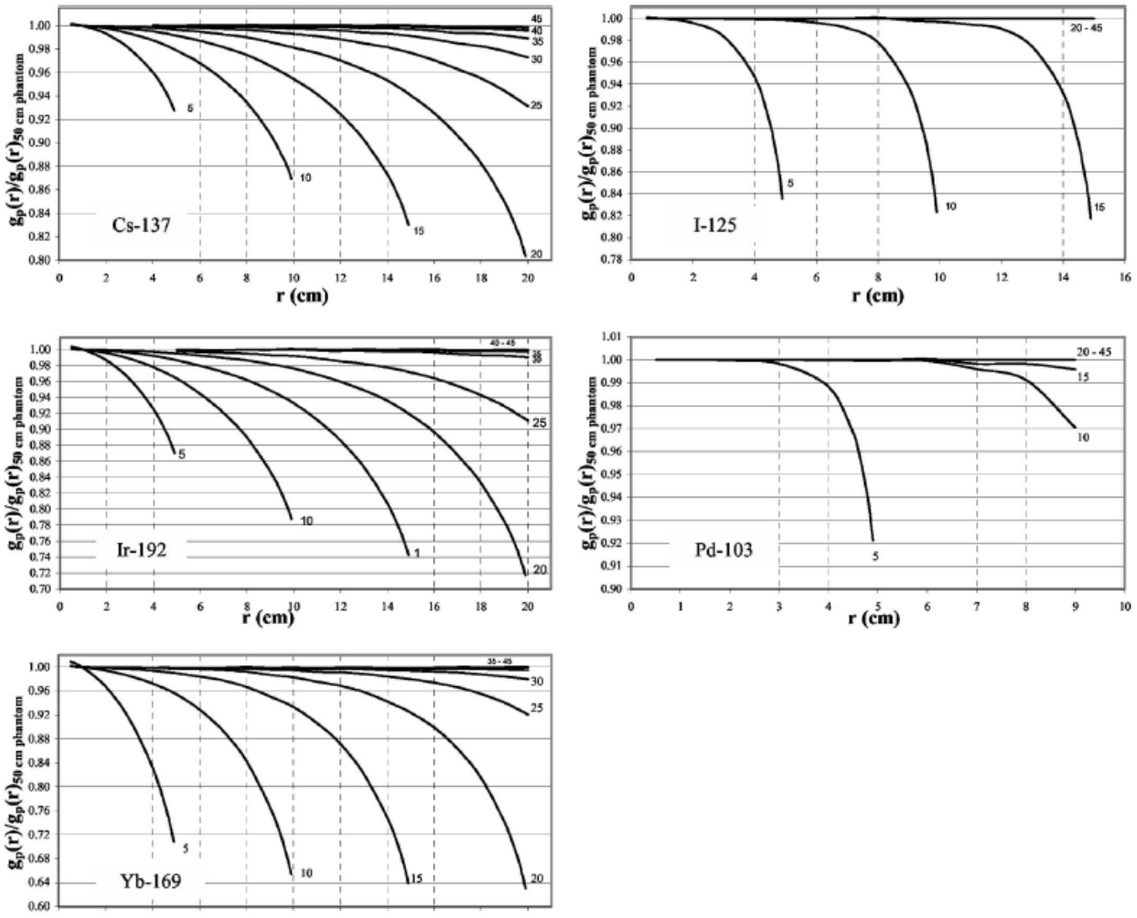

Fig. 3. The ratio of g (r) in different tissues to g (r) in water, for different brachytherapy sources, (i.e. I-125, Cs-137, Ir-192, Pd-103, and Yb-169) (with permission of Med Phys Journal) (Melhus & Rivard, 2006).

In 2008, Song et al performed a study on AAPM TG-43 dose calculation formalism in heterogeneous media for three radioactive seeds (^{125}I, ^{192}Ir and ^{103}Pd). They recommended the modified dose rate constants in different heterogeneities ($\mathbf{\Lambda}'$ (bone)=5.030 and 4.06 cGy/hU for I-125 and Pd-103 respectively) (Song & Wu, 2008).

In 2010 we performed investigation on the effects of tissue inhomogeneities on the dosimetric parameters of a Cs-137 brachytherapy source using the MCNP4C code (Zehtabian et al., 2010). We defined an updated dose rate constant parameter, for Cs-137 source in presence of tissue inhomogenities. The MCNP4C simulations were performed in phantoms composed of water, water-bone and water-air combinations (see Figure 4). The values of dose at different distances from the source in both homogeneous and inhomogeneous phantoms were estimated in spherical tally cells of 0.5 mm radius using the F6 tally. The percentages of dose reductions in presence of air and bone inhomogenities for the Cs-137 source were found to be 4% and 10%, respectively. Therefore, the updated dose rate constant (Λ) will also decrease by the same percentages. The dose rate constant of a single active pellet inside the liquid water phantom was 1.093. The modified values of dose rate constant ($\mathbf{\Lambda}'_a$) for air and bone inhomogenitis were found to be 0.984 and 1.047

respectively (Zehtabian et al., 2010). By comparing our results and Song et al results, it can be easily concluded that such dose variations are more noticeable when using lower energy sources such as Pd-103 or I-125 because of prevail of photoelectric effect.

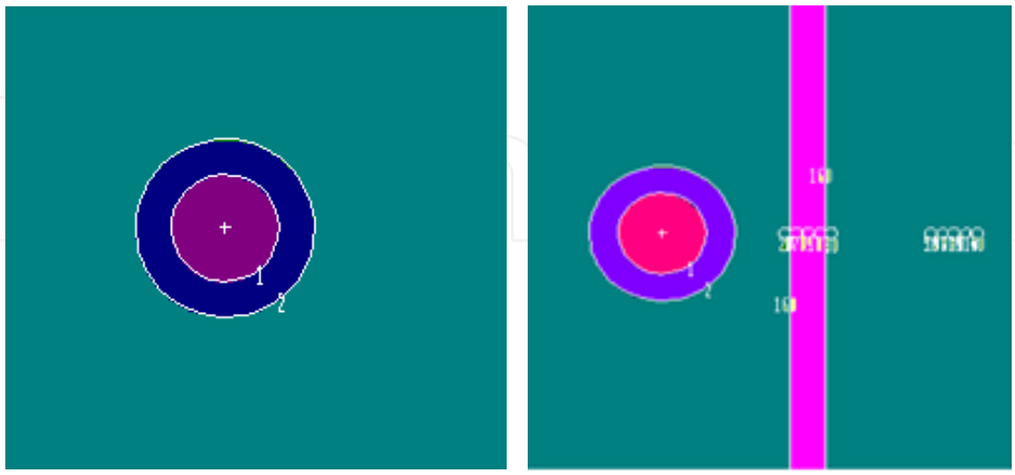

Fig. 4. Simulated geometry of a single active Cs-137 pellet inside the phantom a) uniform water phantom b) Water phantom with inhomogenity (bone or air) (with permission from Iranian Journal of Medical Physics) (Zehtabian et al., 2010).

2.3 InterSource Attenuation (ISA) and influence of applicators

For clinical applications, in which several brachytherapy sources are used in treatment of the patients, the ISA may be significant.

TG-43 parameters of brachytherapy sources are obtained for single brachytherapy sources inside a homogenious water phantom, not considering the effect of other brachytherapy sources (ISA) and the applicators (Markman et al., 2001).

The structures of brachytherapy sources and the applicators are composed of materials with the densities and atomic numbers different from that of water. The photoelectric effect is more dominant in materials with higher atomic numbers, so the TG-43 parameters are different when shielding effects of the applicator and other source are considered in comparison to the water without consideration of these factors (Rivard et al., 2009).

The radio-opaque markers (i.e. silver markers Z=47) which are used in identification during post Implant CT localization in LDR brachytherapy may also cause some inaccuracies in TG-43 dose calculation formalism.

The applicators which are made up of materials with the atomic numbers different from that of water (i.e. stainless steel=26) would also cause some errors in TG-43 parameters.

The difference between the TG-43 parameters of brachytherapy sources in applicator materials are highly dependent on the energy of brachytherapy sources. Consequently not considering the ISA and the applicator effects are more pronounced for brachytherapy sources emitting low energy gamma rays.

Different investigators have studied the shielding effects of other materials (such as the other sources, the applicator components and radio opaque markers) and showed that not

taking the radiation attenuation in such materials into consideration may have significant effect on dose distribution around the brachytherapy sources (Margarida Fragoso, 2004; M. Fragoso et al., 2004; Parsai et al., 2009; Perez-Calatayud et al.,2004, 2005; Sina et al., 2007, 2011; Siwek et al., 1991).

To investigate the shielding effect of the cylindrical vaginal applicator and dummy pellets on TG-43 dosimetry parameters of Cs-137 low dose rate brachytherapy source, we simulated a single active pellet inside the applicator and calculated the geometry parameters of the source (i.e. dose rate constant, radial dose function and anisotropy function) (Sina et al., 2009, 2011a, 2011b).

According to the results of our study, the presence of the applicator does not have any significant effect on the dose rate constant and radial dose function of the source (θ=90°), but the value of anisotropy function differs from unity especially towards the longitudinal axis of the source (θ=0° or θ=180°). Figure 5 shows the anisotropy function of an active pellet inside the applicator (while other pellets are inactive) at different distances from the center of the source. As it is obvious from Figure 5, the value of F (r,θ) are equal to unity at θ=90°, and decrease as the angles reaches 0° and 180°.

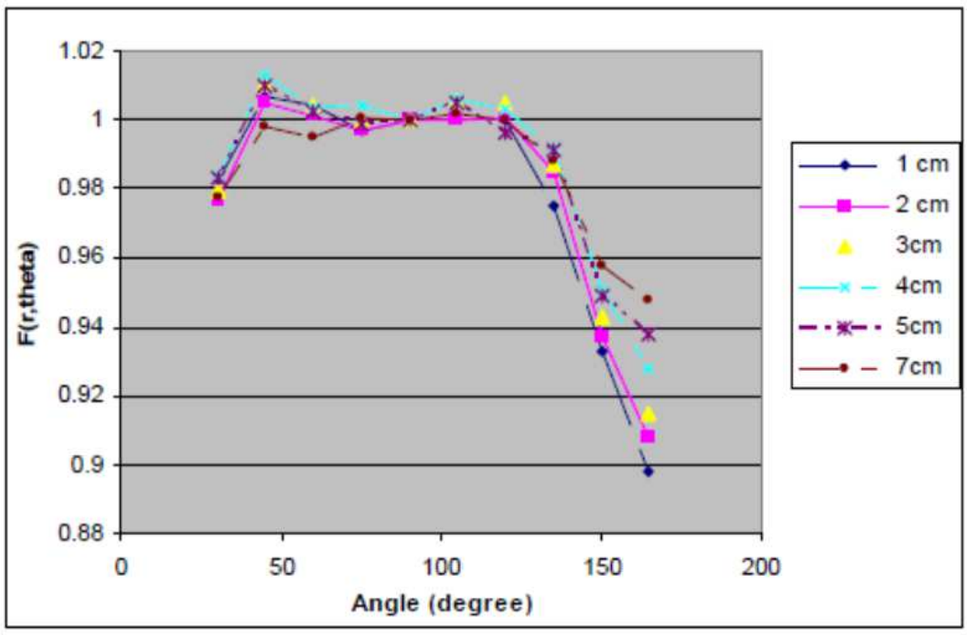

Fig. 5. Comparison of the anisotropy function at different distances and angles from the source (with permission of IJRR). (Sina et al., 2009)

2.4 Phantom size

Differences between radiation scattering for dataset acquisition and patient treatment would also cause some errors in dose calculations based on TG-43 formalism. In actual clinical cases the brachytherapy sources is not placed exactly at the center of the patient's body. Sometimes the radioactive source is placed near the patient's contour, and this change in the scattering condition inside the phantom, would have significant effects on TG-43 parameters of the sources.

The percentages of difference in TG-43 parameters are highly affected by energy of the photons emitted from brachytherapy sources, and the amount of missing tissue (the phantom size).

Several investigators has studied the phantom size as an important point in BT dosimetry study is the phantom size involved either in MC calculations or experimental measurements (Anagnostopoulos et al., 1991, 2003; Herbold et al., 1988; Karaiskos et al., 2003; Sakelliou et al., 1992; Tiourina, 1995). Williamson 1991, showed 5%–10% differences at distances greater than 5cm from a ^{192}Ir source comparing the dose in an unbounded liquid–water and a phantom of of nearly 20*20*20 cm^3 (Williamson, 1991). Venselaar *et al.* have investigated the influence of phantom size on dose by changing the water level in a cubic water tank for ^{137}Cs, ^{60}Co and ^{192}Ir sources (Venselaar et al., 1996). They obtained significant differences in the dose between experiments with different phantom sizes. Karaiskos *et al.* investigated the effect of water spherical phantom size on ^{192}Ir MicroSelectron HDR source of diameters ranging from 10 to 50 cm on the radial dose function, g (r), at radial distances near phantom boundaries, both experimentally and theoretically, and observed up to 25% differences at the points near the phantom boundaries (Karaiskos et al., 2003). It is better to take such differences into account in the dose calculations of the treatment planning softwares in clinical cases which the sources are located near the phantom boundaries.

Pe´rez-Calatayud et al verified the influence of phantom size on the radial dose function of different brachytherapy sources using GEANT4 code. They found that a 15 cm radius water phantom ensures full scatter conditions up to 10 cm from the low energy photon emitting brachytherapy sources like ^{103}Pd, and ^{125}I (Perez-Calatayud, 2004). They also suggested the unbounded phantom radius of 40cm for ^{137}Cs and ^{192}Ir sources.

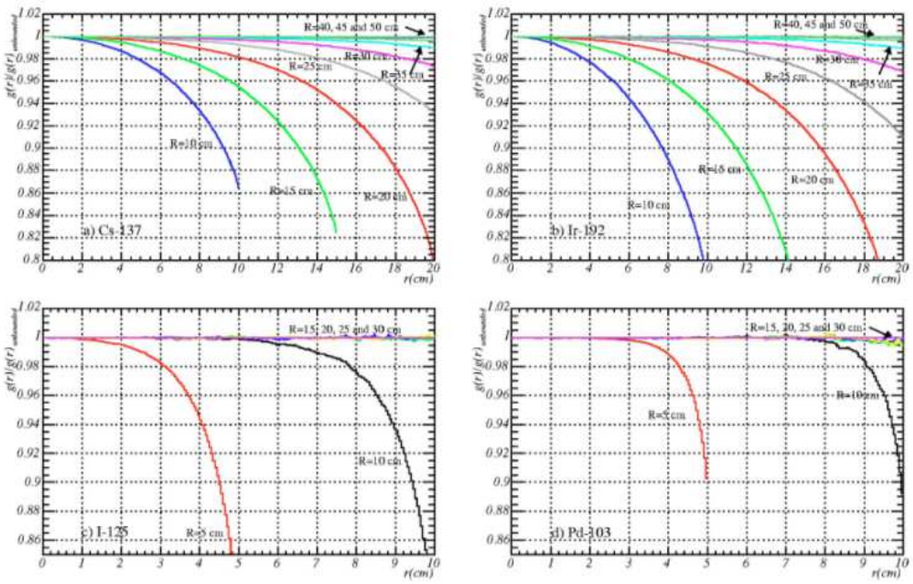

Fig. 6. Ratio between the radial dose function for a phantom size R and the radial dose function for an unbounded phantom, for ^{137}Cs, ^{192}Ir, ^{125}I and ^{103}Pd point sources and for various phantom sizes (Perez-Calatayud, 2004).

Melhus et al 2006, also compared the g (r) values for different phantom sizes with the values of g (r) for a phantom size of R=50cm using MCNP5 Monte Carlo code and found that the MCNP5 results were in agreement with the GEANT4 code (see Figure 7).

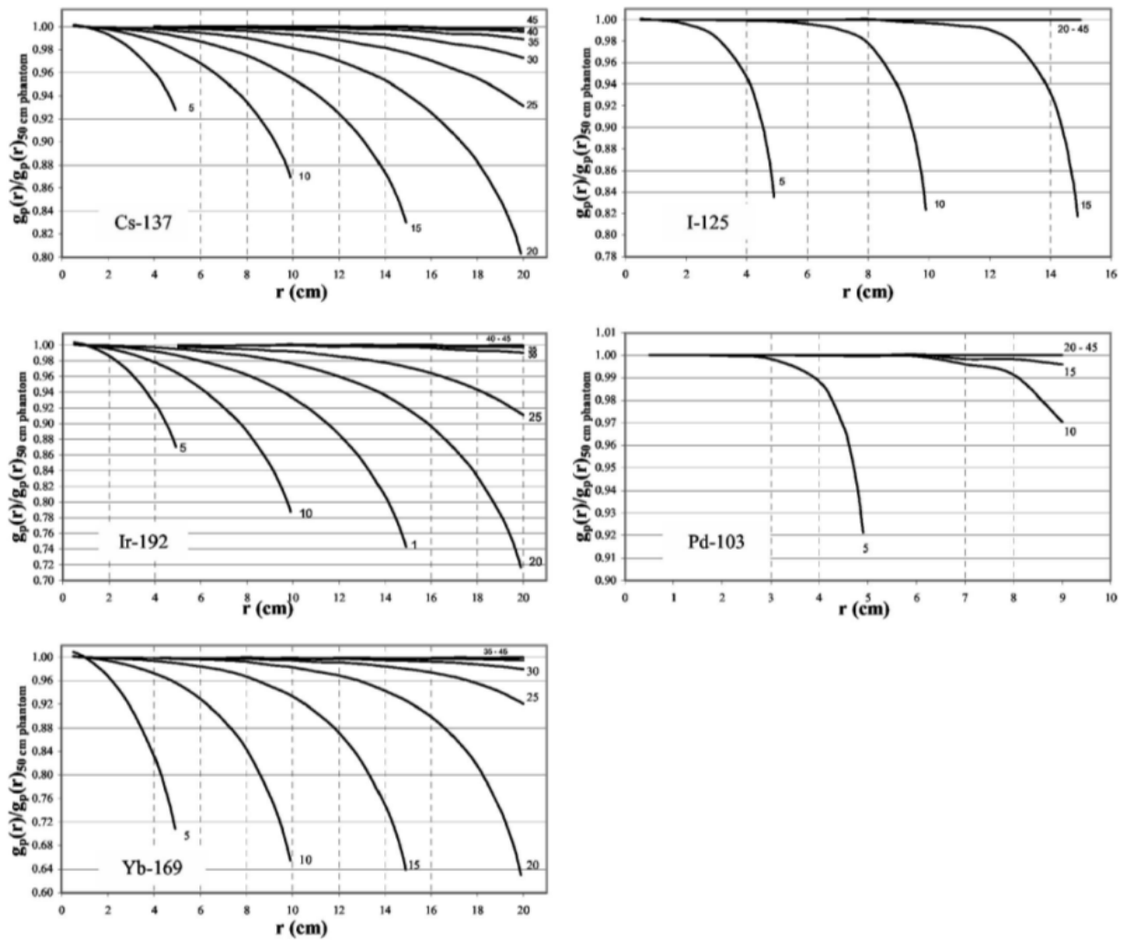

Fig. 7. Comparison of g (r) values for phantoms of different sizes with the phantom of R=50cm, for different brachytherapy sources. (Melhus & Rivard, 2006)

3. Conclusions

Today, most of brachyherapy treatment planning systems are based on the recommendations of AAPM Task Group #43 dose calculation formalism (TG-43). The tabulated data including TG-43 parameters of the brachytherapy sources which are obtained experimentally or theoretically, are used as the input data of the treatment planning softwares. The TG-43 parameters are obtained by positioning the source at the center of a fixed volume homogeneous water phantom, not considering the different scattering and attenuation of the photons in other tissues, the phantom size and the ISA and the applicator shielding effects.

Such limitations would affect the outcome of the treatment planning softwares. It is recommended that such factors be taken into considerations as much as possible, by applying some correction factors.

4. References

Anagnostopoulos, G.; Baltas, D.; Karaiskos, P.; Pantelis, E.; Papagiannis, P. & Sakelliou, L. (2003). An analytical dosimetry model as a step towards accounting for

inhomogeneities and bounded geometries in 192Ir brachytherapy treatment planning. *Phys. Med. Biol.* , 48, 1625-1647.

Angelopoulos, A.; Perris, A.; Sakellariou, K.; Sakelliou, L.; Sarigiannis, K. & Zarris, G. (1991). Accurate Monte Carlo calculations of the combined attenuation and build-up factors, for energies (20–1500 keV) and distances (0–10 cm) relevant in brachytherapy,. *Phys. Med. Biol.* , 36, 763–778.

Fragoso, M. (2004). Application of Monte Carlo Techniques for the Calculation of Accurate Brachytherapy Dose Distributions., University of London, London,UK.

Fragoso, M.; Love, P.A.; Verhaegen, F.; Nalder, C.; Bidmead, A.M.; Leach, M., et al. (2004). The dose distribution of low dose rate Cs-137 in intracavitary brachytherapy: comparison of Monte Carlo simulation, treatment planning calculation and polymer gel measurement. *Phys Med Biol*, 49 (24), 5459-5474.

Herbold, G.; Hartmann, G.; Treuer, H. & Lorenz, W.J. (1988). Monte Carlo calculation of energy build-up factors in the range from 15 keV to 100 keV, with special reference to the dosimetry of 125I seeds. *Phys. Med. Biol.* , 33, 1037-1053. ICRU, I.C.o.R.U.a.M.R.N. (1989). Tissue substitutes in radiation dosimetry and measurement.

Karaiskos, P.; Angelopoulos, A.; Pantelis, E.; Papagiannis, P.; Sakelliou, L.; Kouwenhoven, E., et al. (2003). Monte Carlo dosimetry of a new 192Ir pulsed dose rate brachytherapy source. *Med Phys*, 26 (4), 9-16.

Khan, F.M. (2003). The Physics of Radiation Therapy (Third ed.). Philadelphia: Lippimcott Williams and Wilkins.

Liu, L., Prasad, S.C., & Bassano, D.A. (2004). Determination of 137Cs dosimetry parameters according to the AAPM TG-43 formalism. *Med Phys*, 31 (3), 477-483.

Markman, J.; Williamson, J.F.; Dempsey, J.F. & Low, D.A. (2001). On the validity of the superposition principle in dose calculations for intracavitary implants with shielded vaginal colpostats. *Med Phys*, 28 (2), 147-155.

Meigooni, A.S.; Rachabatthula, V.; Awan, S.B. & Koona, R.A. (2005). Comment on "Update of AAPM Task Group no. 43 report: A revised AAPM protocol for brachytherapy dose calculations". *Med Phys*, 32 (6), 1820-1821; author reply 1822-1824.

Meigooni, A.S.; Zhang, H.; Perry, C.; Dini, S.A. & Koona, R.A. (2003). Theoretical and experimental determination of dosimetric characteristics for brachyseed Pd-103, model Pd-1, source. *Appl Radiat Isot*, 58 (5), 533-541.

Melhus, C.S. & Rivard, M.J. (2006). Approaches to calculating AAPM TG-43 brachytherapy dosimetry parameters for 137Cs, 125I, 192Ir, 103Pd, and 169Yb sources. *Med Phys*, 33 (6), 1729-1737.

Nath, R.; Anderson, L.L.; Luxton, G.; Weaver, K.A.; Williamson, J.F. & Meigooni, A.S. (1995). Dosimetry of interstitial brachytherapy sources: recommendations of the AAPM Radiation Therapy Committee Task Group No. 43. American Association of Physicists in Medicine. *Med Phys* 22 (2), 206-234.

Nucletron. (1998). General information. Netherlands.

Parsai, E.I.; Zhang, Z. & Feldmeier, J.J. (2009). A quantitative three-dimensional dose attenuation analysis around Fletcher-Suit-Delclos due to stainless steel tube for high-dose-rate brachytherapy by Monte Carlo calculations. *Brachytherapy*, 8 (3), 318-323.

Perez-Calatayud, J.; Granero, D. & Ballester, F. (2004). Phantom size in brachytherapy source dosimetric studies. *Med Phys*, 31 (7), 2075-2081.

Perez-Calatayud, J.; Granero, D.; Ballester, F. & Lliso, F. (2005). A Monte Carlo study of intersource effects in dome-type applicators loaded with LDR Cs-137 sources. *Radiother Oncol*, 77 (2), 216-219.

Perez-Calatayud, J.; Granero, D.; Ballester, F.; Puchades, V. & Casal, E. (2004). Monte Carlo dosimetric characterization of the Cs-137 selectron/LDR source: evaluation of applicator attenuation and superposition approximation effects. *Med Phys*, 31 (3), 493-499.

Rivard, M.J.; Butler, W.M.; DeWerd, L.A.; Huq, M.S.; Ibbott, G.S.; Meigooni, A.S. et al. (2007). Supplement to the 2004 update of the AAPM Task Group No. 43 Report. *Med Phys*, 34 (6), 2187-2205.

Rivard, M.J.; Coursey, B.M.; DeWerd, L.A.; Hanson, W.F.; Huq, M.S.; Ibbott, G.S. et al. (2004). Update of AAPM Task Group No. 43 Report: A revised AAPM protocol for brachytherapy dose calculations. *Med Phys*, 31 (3), 633-674.

Rivard, M.J.; Venselaar, J.L. & Beaulieu, L. (2009). The evolution of brachytherapy treatment planning. *Med Phys*, 36 (6), 2136-2153.

Sakelliou, L.; Sakellariou, K.; Sarigiannis, K.; Angelopoulos, A.; Perris, A. & Zarris, G. (1992). Dose rate distributions around 60Co, 137Cs, 198Au, 192Ir, 241Am, 125I (models 6702 and 6711) brachytherapy sources and the nuclide 99Tcm. *Phys. Med. Biol*., 37, 1859–1872.

Sina, S. (2007). Simulation and Measurement of Dosimetric Parameters for ^{137}Cs Brachytherapy Source, Based on TG-43 Protocol by TLD and Monte Carlo. Shiraz univercity, Shiraz

Sina, S.; Faghihi, R.; Meigooni, A.S.; Mehdizadeh, S.; Mosleh Shirazi, M.A. & Zehtabian, M. (2011a). Impact of the vaginal applicator and dummy pellets on the dosimetry parameters of Cs-137 brachytherapy source. *Journal of Applied Clinical Medical Physics*, 12 (3), 183-193.

Sina, S.; Faghihi, R.; Meigooni, A.S.; Mehdizadeh, S.; Zehtabian, M. & Mosleh Shirazi, M.A. (2009). Simulation of the shielding effects of an applicator on the AAPM TG-43 parameters of CS-137 Selectron LDR brachytherapy sources. *Iran. J. Radiat. Res*, 7 (3), 135-140.

Sina, S.; Faghihi, R.; Zehtabian, M. & Mehdizadeh, S. (2011b). Investigation of anisotropy caused by cylinder applicator on dose distribution around Cs-137 brachytherapy source using MCNP4C code. *Iran. J. of Med. Physics*, 8 (2 (31)), 57-65.

Siwek, R.A.; Obrien, P.F. & Leung, P.M.K. (1991). Shielding effects of Selectron applicator and pellets on isodose Distributions. *Radiother. Oncol*., 20, 132–138.

Song, G., & Wu, Y. (2008, Jun). In A Monte Carlo Interstitial Brachytherapy Study for AAPM TG-43 Dose Calculation Formalism in Heterogeneous Media. Paper presented at the 2nd International Conference on Bioinformatics and Biomedical Engineering, 2008. ICBBE 2008.

Tiourina, T.B.; Dries, W.J.F. & van der Linden, P.M. (1995). Measurements and calculations of the absorbed dose distribution around a 60Co source. *Med Phys*, 22 (5), 549–554.

UT-Battelle, & LLC. (2000). Rsic Computer Code Collection MCNP4C. New Mexico: Los Alamos National Laboratory.

Venselaar, J.L.M., Van der Giessen, P.H., & Dries, W.J.F. (1996). Measurement and calculation of the dose at large distances from brachytherapy sources: Cs-137, Ir-192, and Co-60. *Med. Phys.*, 23, 537-543.

Williamson, J.F. (1991). Comparison of measured and calculated dose rates in water near I-125 and Ir-192 seeds. *Med Phys*, 18 (4), 776-786.

Zehtabian, M.; Faghihi, R. & Sina, S. (2010). Comparison of dosimetry parameters of two commercially available Iodine brachytherapy seeds using Monte Carlo calculations. *Iran. J. Radiat. Res*., 7 (4), 217-222.

Zehtabian, M.; Faghihi, R.; Sina, S. & Noorizadeh, A. (2010). Investigation of the Effects of Tissue Inhomogeneities on the Dosimetric Parameters of a Cs-137 Brachytherapy Source using the MCNP4C Code. *Iran. J. of Med. Physics*, 7 (3 (28)), 15-20.

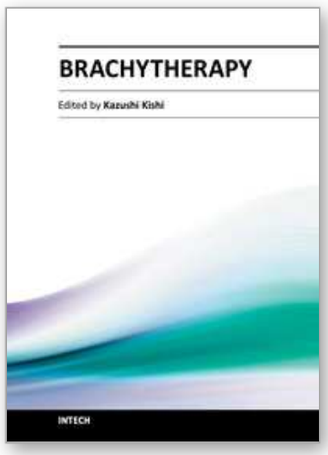

Brachytherapy
Edited by Dr. Kazushi Kishi

ISBN 978-953-51-0602-9
Hard cover, 128 pages
Publisher InTech
Published online 25, April, 2012
Published in print edition April, 2012

Importance of brachytherapy is currently increasing in cancer therapy. In brachytherapy each treatment is best fitted by physician's' hand, and appropriate arrangement and selection of radiation sources facilitates the fitting. This book is full of essences to make a breakthrough in radiation oncology by brachytherapy. I hope this book will encourage all people related. Contents 1: problem of currently popular dosimetric method; 2: Monte Carlo dose simulation of ruthenim-106/rhodium-106 eyes applicators; 3. Progress in Californium-252 neutron brachytherapy; 4. Clinical aspect of endobronchial brachytherapy in central airway tumor obstruction; 5. Review from principle and techniques of Iodine-125 production at nuclear reactor plant to their clinical practive in prostate cancer treatment; 6. Stereotactic Brachytherapy for Brain Tumors using Iodine-125 seed; 7. A brachytherapy procedure with organ-sparing hyaluronate gel injection for safe and eradicative reirradiation.

INTECH
open science | open minds

InTech Europe
University Campus STeP Ri
Slavka Krautzeka 83/A
51000 Rijeka, Croatia
Phone: +385 (51) 770 447
Fax: +385 (51) 686 166
www.intechopen.com

InTech China
Unit 405, Office Block, Hotel Equatorial Shanghai
No.65, Yan An Road (West), Shanghai, 200040, China
中国上海市延安西路65号上海国际贵都大饭店办公楼405单元
Phone: +86-21-62489820
Fax: +86-21-62489821

IntechOpen